Colloquia: La Thuile 2016

Status of the GERDA experiment

E. Medinaceli on behalf of the GERDA Collaboration

INFN & Università di Padova - via Marzolo 8, 35100 Padova, Italy

Summary. — The GERDA experiment is designed to search for neutrinoless double beta decay ($0\nu\beta\beta$) using ^{76}Ge, therefore asses the nature of neutrinos (Dirac or Majorana). In the so-called Phase I, with an exposure of 21.6 kr yr, GERDA reached a background index (BI) of 10^{-2} cts/(keV kg yr) at 90% CL No signal was found during this phase and a lower limit on the process half-life of 2.1×10^{25} yr was derived (90% CL). GERDA is currently being upgraded to its Phase II, where the ^{76}Ge mass will be double, and it is expected to reduce by an order of magnitude the BI. For $0\nu\beta\beta$ half-lives at the order of 10^{26} yr will be derived in the absence of signal. The experimental techniques used by GERDA will be depicted and the most relevant results from Phase I will be shown; as well as details on the upgrades of Phase II, including the status of the additional detectors deployed recently, and the new background reduction techniques using the active liquid Argon veto.

1. – The GERDA experiment

The GERmanium Detector Array (GERDA) experiment search for the neutrino-less double beta decay $0\nu\beta\beta$ ($(Z, A) \rightarrow (Z + 2, A) + 2e^-$) of ^{76}Ge, predicted by extensions of the Standard Model. This process violates by two units the lepton number conservation, and is mediated by neutrinos having a Majorana mass component being equal to their anti-particles. This is a very rare decay and the half-live $T_{1/2}^{0\nu\beta\beta}$ (exceeding 10^{25} yr, *i.e.* $\ll 0.1$ event/(keV kg yr)); therefore extremely low background is required to search for its signature. $T_{1/2}^{0\nu\beta\beta}$ is connected to the effective Majorana neutrino mass $m_{\beta\beta}$, so by measuring $m_{\beta\beta}$ the mass of the lightest neutrino mass can be constrained and limits on the neutrino mass hierarchy could be inferred.

The $0\nu\beta\beta$ signature is the monochromatic line at the $Q_{\beta\beta}$-value of the decay located at the tail of the $2\nu\beta\beta$ spectrum. High-energy resolution is a requirement to identify this peak. To do so, GERDA uses an array of high-purity germanium (HPGe) detectrs, isotopically enriched to $\sim 86\%$ with the ^{76}Ge isotope. To increase the detection efficiency HPGe detectors are also used as sources of β-decays being the $0\nu\beta\beta$ $Q_{\beta\beta}$ for ^{76}Ge at 2039 keV. The usage of this kind of detectors allows industrial support because
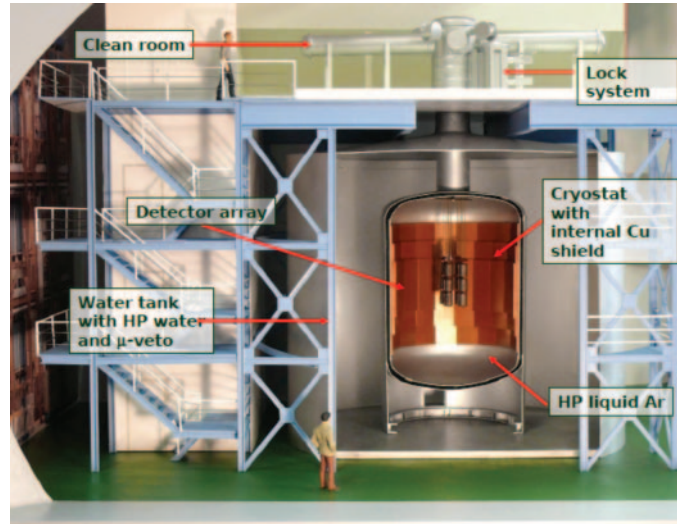
Fig. 1. – GERDA detector facility at INFN's Gran Sasso underground lab. The different detector parts are indicated: the cryostat which contains the HPGe detectors array, and the high-purity (HP) liquid Argon volume of $64\,m^3$; the muon veto composed of a vessel containing $590\,m^2$ of high-purity water; the clean room and the lock system where detectors are assembled and deployed inside the cryostat [3].

a established detector technology exists. GERDA uses to types of HPGe detectors with slightly different geometries and physical performances. Among them are the so-called Semi-Coaxial (Coaxial) detectors refurbished from HdM [1] and IGEX [2] experiments; and the new Broad Energy Germanium detectors (BEGe). The mean energy resolution of HPGe detectors used in GERDA is $\sim 0.1\%$ at $Q_{\beta\beta}$.

The experimental concept design consists in the deployment of bare Germanium detectors in liquid Argon (LAr) and pure water, to prevent external backgrounds [3]. HPGe detectors are deployed in a $64\,m^3$ cryostat filled with LAr. The cryostat is embedded in a vessel containing $590\,m^2$ ultra-pure water providing additional shielding. The water tank is instrumented with photo-multipliers and Cerenkov light emission is used to detect cosmic ray muons. A complementary plastic scintillator muon veto is placed on the roof of the detector, above the neck of the deployment lock system [3]. Figure 1 is the rendering of the GERDA detector facility. GERDA is located at Hall A of the INFN's national underground laboratory of Gran Sasso, Italy, with a total overburden of $3500\,m.w.e.$ In GERDA are implemented pulse shape discrimination techniques of the charge signal [4,5] to improve the experimental sensitivity.

2. – GERDA Phase I results

GERDA Phase I is defined as the data taking period from November 2011 to December 2013. The run had an 88% duty cycle and during this period weekly ^{228}Th calibrations and constant monitoring with test pulser were performed. The total exposure was $21.6\,kg\,yr$ with a total mass of $14.6\,kg$ of Coaxial detectors plus $6.0\,kg$ of BEGe detectors. During this phase the LAr volume was used as a passive veto material. A blinding analysis technique was used removing from raw data the region of interest (ROI) $\pm 40\,keV$

around $Q_{\beta\beta}$. The data selection applied consists in: a cut of unphysical events with a $< 0.1\%$ misidentification capability; a muon veto rejection of 99.1% efficiency; a selection criteria to discard anti-coincidences (signal in more than one detector) achieving a negligible value of random coincidences; and a further selection to suppress the cascade of low energy ^{214}Bi and high energy α component of ^{214}Po with an efficiency of $\sim 50\%$ [6]. Energy resolution (average FWHM) for Phase I amounts to 4.8 keV at $Q_{\beta\beta}$.

2˙1. *Background model*. – A background model was obtained taking into account the several contributions on the basis of material screening or what is determined by the observation of characteristic structures in the energy spectrum. The main contribution comes from a radioactive component of ^{228}Th and ^{226}Ra of the detector holders; ^{42}Ar and α contamination on the surface of the detectors. Figure 2 is the energy spectrum where with a black solid line the best fit is shown for the "minimum model" of the GOLD-coax data set (17.9 kg yr using the HPGe Coaxial detector) depicted with black dots. The contributions of different isotopes and the α contamination are also shown, lines 2014 keV of ^{108}Tl, and 2119 keV ^{214}Bi were excluded. The $2\nu\beta\beta$ spectrum plotted with a green solid line, is also considered as a background source for the $0\nu\beta\beta$ signal. The lower panel in the plot shows the ratio between the data and the prediction of the best fit model together with the smallest intervals of 68% (green band), 95% (yellow band) and 99.9% (red band) probability for the ratio assuming the best fit parameters [7].

The model was used to predict the intensity and the spectral shape of the background in the region of interest around $Q_{\beta\beta}$, before the actual unblinding. No peak was expected at ROI and the mean background index of 10^{-2} counts/(keV kg yr) was derived for that region. The number of events expected predicted by the background model for the $Q_{\beta\beta}$ region ranges from 8.6 to 10.3 events, according to the minimum (ploted in fig. 2) or maximum model (not shown) [7].
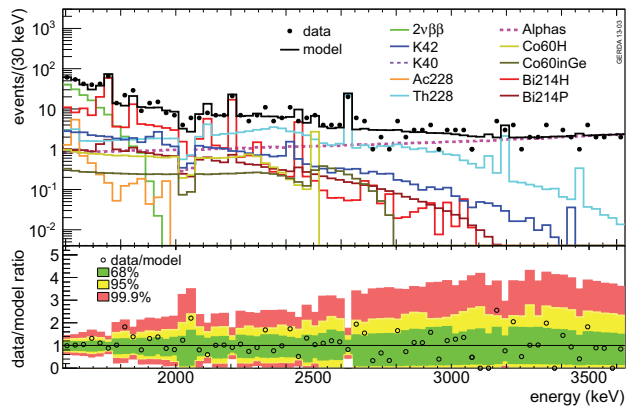

Fig. 2. – Background decomposition to the best fit minimum model of the GOLD-coax data set, shown with a black solid line. The contribution of different isotopes is also shown. The green solid line represents the $2\nu\beta\beta$ contribution, and the experimental energy spectrum is represented with black markers. Circular markers in the lower panel in the plot shows the ratio between the data and the prediction of the best fit model, the coloured bands represents the probability intervals, 68% interval (green band), 95% (yellow band) and 99.9% (red band) [7].

2˙2. $2\nu\beta\beta$ *results*. – The GOLD-coax data set was used for this analysis and the $2\nu\beta\beta$ spectrum was fitted with the background model [6] using the binned Maximum Likelihood approach. The half-live of the decay derived is $T_{1/2}^{2\nu\beta\beta} = (1.926 \pm 0.0095) \times 10^{21}$ yr; more details about the statistical procedure can be found in ref. [8].

2˙3. $0\nu\beta\beta$ *results*. – For this analysis Pulse Shape Discrimination (PSD) techniques were used to further eliminate the background. Two independent methods are applied according to the detector type. For Coaxial detectors artificial Neural Networks (ANN) are used, trained with proxies of different kinds of events easily recognizable; calibration data of ^{228}Th spectrum is used for this procedure. Events of ^{208}Tl line, which deposit energy is in a single point, called Single Side Events (SSE) are considered representative of signal-like events; while events whose energy deposition that does not occur in a single point, like the ^{212}Bi line, so-called Multiple Site Events (MSE) behaves as background. The classificator selection cut is adjusted to have $90_9^{+5}\%$ of survival probability.

For the BEGe detectors a cut is applied on the variable A/E, A stands for the amplitude of the current pulse measured in the detector, and E represents the energy evaluated for the event. A/E has a high capability of distinguishing SSE from MSE, and superficial events (p$^+$ with its characteristic fast current pulse, and n$^+$ with its characteristic low-energy deposition). In this case the acceptance of $0\nu\beta\beta$ events is $(92 \pm 2)\%$ while for $2\nu\beta\beta$ is $(91 \pm 5)\%$ [4,5].

The total exposure reached for the $0\nu\beta\beta$ results is 21.6 kg yr. After the full chain analysis was settled, considering calibrations, data selection, and PSD analysis the ROI around the $Q_{\beta\beta}$ was unblinded. The background index (BI) after the application of the PSD is BI $= 0.01$ cts/(keV kg yr) in the ROI. The expected signal events considering the background model and the PSD analysis is (5.9 ± 1.4) cts in the $\pm 2\sigma$ interval; the background expected events, considering the PSD analysis is (2.0 ± 0.3) cts in the $\pm 2\sigma$ interval. Figure 3 shows the combined energy spectrum around $Q_{\beta\beta}$ of all HPGe detectors with (solid) and without (open) PSD. The lower panel (bottom), shown the region 1930 to 2190 keV used for the background interpolation. The upper panel (top) shows the spectrum zoomed in to $Q_{\beta\beta}$ superimposed with the expectation (with PSD selection). Seven events were observed in the region $Q_{\beta\beta} \pm 5$ keV before PSD. No excess of events beyond the expected background is observed, this interpretation is strengthened by the pulse shape analysis, and here after are results quoted are referred after the pulse shape analysis. To derive the signal strength $N^{0\nu}$ and a frequentist coverage interval a profile likelihood fit was applied. The fitted function consists of a constant term for the background and a Gaussian peak for the signal with a mean value at $Q_{\beta\beta}$ (blue curve) and standard deviation σ_E according to the expected resolution, see fig. 3. In the same plot the red segmented curve represents the KK claim [9] which is strongly disfavoured by this analysis. The likelihood ratio was only evaluated for the physically allowed region $T_{1/2}^{0\nu} > 0$. Systematics uncertainties are folded in with a Monte Carlo approach which takes into account correlations. The best fitted value is $N^{0\nu} = 0$, no excess of signal events above the background. The limit on the half-life including systematic uncertainties is [6]

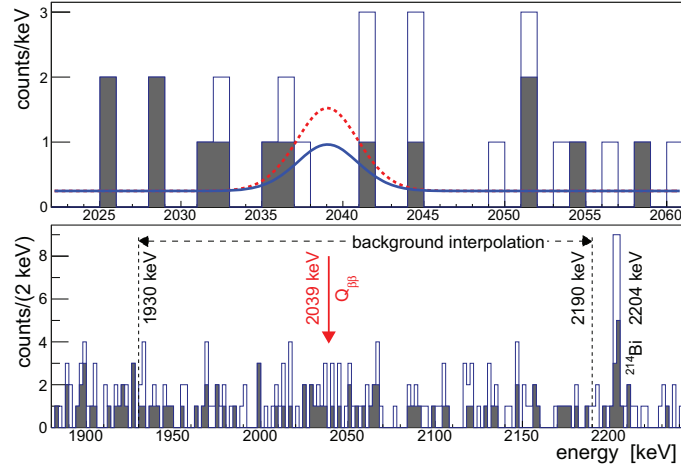$$T_{1/2}^{0\nu} > 2.1 \times 10^{25} \text{ yr} \quad (90\% \text{ CL}).$$

Fig. 3. – Combined energy spectrum of GERDA Phase I without (with) PSD is shown by the open (filled) histogram. The lower panel shows the region used for the background interpolation. In the upper panel, the spectrum zoomed to $Q_{\beta\beta}$ is superimposed with the expectations (with PSD selection). The blue curve is the signal fit [2], while the red segmented curve is the result claimed by [9].

3. – GERDA Phase II status

After Phase I, several improvements on the detector instrumentation were implemented in order to further reduce the residual background by $\sim 10\times$ to obtain a BI ~ 0.001 cts/(keV kg yr). To reach this level, among the new detector and software features are: reducing the detector holders mass; upgrading the front-end read-out and cabling, including the high voltage one; improving the PSD capabilities; increasing the energy resolution [10]; and instrumenting the LAr veto. Liquid Argon veto was equipped with curtains of scintillation strips coated with wavelength shifter, coupled to SiPMs and 3" PMTs at the top and bottom of the detector array; allowing together to the PSD techniques a strong background reduction at $Q_{\beta\beta}$.

The commissionig of Phase II was done using a single string of three BEGe detectors running with 15 PMTs and 7 SiPMs for 25 hours. During commissioning calibrations were done using the ^{228}Th isotope, fig. 4 shows the energy spectrum obtained. In the plot are indicated the datasets corresponding to different background reduction steps: the first data selection is done applying the anti-coincidence (AC) cut, plotted with a gray histogram; the red line represent the data after the AC cut plus the PSD selection; blue histogram represent data after the AC cut plus the LAr veto selection; the light blue histogram show the final dataset obtained by the application of all the background reduction criteria, namely the AC cut plus PSD, and LAr veto selection. It was preliminary evaluated while commissioning that a high background reduction at the order of $\sim 100\times$ could be obtained combining the LAr veto results with the PSD techniques. Commissioning of Phase II proceed with an assembly of 5 strings of BEGe detectors, fig. 5 shows the energy spectrum of calibration runs using isotope ^{228}Th, in the plot are shown the results of 7 HPGe detectors. The energy resolution (FWHM) was evaluated for both detector types using the full energy deposition peak of the spectrum at 2.6 MeV; the measurements of this peak are highlighted in an insertion of the figure. The results obtained are, for BEGeS ~ 3 keV, and ~ 4 keV for Coaxial detectors.
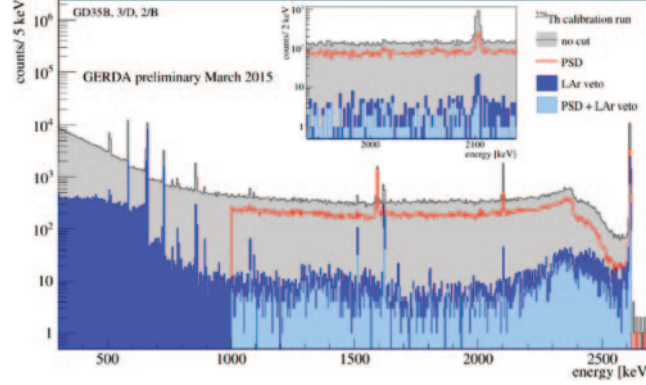
Fig. 4. – Energy spectrum of the calibration data using ^{228}Th isotope; different background reduction steps are indicated. Data selected with the anti-coincidence (AC) cut is plotted with a grey histogram; the red line represent the data after the AC cut plus the PSD selection; blue histogram represent data after the AC plus PSD and LAr veto selections; light blue histogram show the final data selected after the application of the AC cut plus PSD, and LAr veto selection.
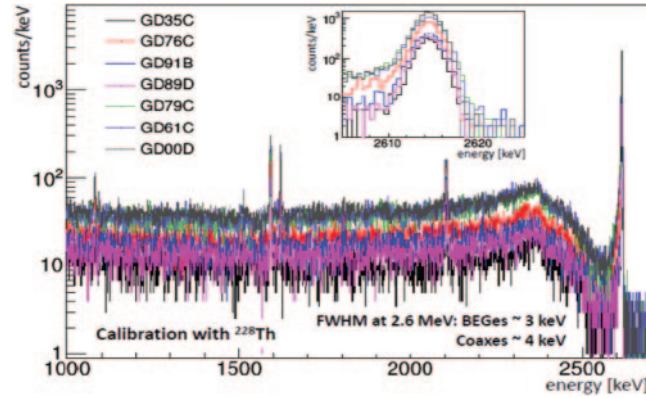

Fig. 5. – Energy spectra of calibrations performed with ^{228}Th measured with 7 HPGe detector. The full energy deposition peak at 2.6 MeV was used as a proxy for the determination of the energy resolution of the detectors. A zoom in of the measurements corresponding to this proxy is inserted in the small box.

Commissioning finished showing a fully operational LAr veto, all 40 HPGe diodes show a stable behaviour and good energy resolution (at the same level of the resolution obtained on Phase I). Also during this commissioning runs it was demonstrated that the background reduction was improved.

Since December 2015 GERDA is running Phase II, with an increased mass of around 20 kg (30 new HPGe detectors [11]), to increase the experimental sensitivity of the $0\nu\beta\beta$ half-live to about $T^{0\nu}_{1/2} \sim 10^{26}$ yr by collecting an exposure of ~ 100 kr yr.

REFERENCES

[1] HEIDELBERG-MOSCOW COLLABORATION (KLAPDOR-KLEINGROTHAUS H. V. *et al.*), *Eur. Phys. J. A*, **12** (2001) 147.
[2] IGEX COLLABORATION (AALSETH C. E. *et al.*), *Phys. Rev. D*, **65** (2002) 092007.
[3] GERDA COLLABORATION (ACKERMANN K. H. *et al.*), *Eur. Phys. J. C*, **73** (2013) 2330.
[4] GERDA COLLABORATION (AGOSTINI M. *et al.*), *Eur. Phys. J. C*, **73** (2013) 2583.
[5] DUSAN B. *et al.*, *JINST*, **4** (2009) 10007.
[6] GERDA COLLABORATION (AGOSTINI M. *et al.*), *Phys. Rev. Lett.*, **111** (2013) 122503.
[7] GERDA COLLABORATION (AGOSTINI M. *et al.*), *Eur. Phys. J. C*, **74** (2014) 2764.
[8] GERDA COLLABORATION (AGOSTINI M. *et al.*), *Eur. Phys. J. C*, **75** (2015) 416.
[9] KLAPDOR-KLEINGROTHAUS H. V. *et al.*, *Phys. Lett. B*, **586** (2004) 198.
[10] AGOSTINI M. *et al.*, *Eur. Phys. J. C*, **75** (2015) 255.
[11] GERDA COLLABORATION (AGOSTINI M. *et al.*), *Eur. Phys. J. C*, **75** (2015) 39.